# RADIATION-GUIDED P-SELECTIN TARGETED TUMOR IMAGING IN A LUNG TUMOR MODEL

By

Ghazal Hariri

Thesis

Submitted to the Faculty of the

Graduate School of Vanderbilt University

in partial fulfillment of the requirements

for the degree of

MASTER OF SCIENCE

in

Biomedical Engineering

May, 2007

Nashville, Tennessee

Approved:

Professor Dennis E. Hallahan

Professor Todd D. Giorgio

ACKNOWLEDGEMENTS

I would like to thank my advisor, Dr. Dennis Hallahan, for supporting me and teaching me the value of collaboration and leadership. It has been a wonderful experience working with him. I would also like to thank Dr. Todd Giorgio for his time and advice on this project. I am grateful for the many hours of help and insightful conversations from graduate students Hailun Wang and Sam Kuhn. I would also like to acknowledge the generous advice and guidance from Dr. Zhaozhong Han and Allie Fu.

This work would not have been possible without the support from NIH grant number CA114201-01. I would like to thank Dr. Ray Mernaugh, Dr. Ying Zhang, Dr. Ling Geng, Dr.Todd Peterson and Dr. Noor Tantawy for their collaboration on this project. Additionally, I would like to thank Vanderbilt University's Institute of Imaging Science for providing access to their imaging equipment and for assistance in image processing. Antibody conjugated with DTPA was generously provided by Dr. Martin Brechbiel at the NIH.

Finally, I am forever grateful for the love and support of my mother, father and sister. I would also like to thank my grandmother for her unconditional love and support and for making me believe I can accomplish anything. This work was truly inspired by her tremendous strength, courage and faith in life.

TABLE OF CONTENTS

LIST OF FIGURES

# CHAPTER I

## INTRODUCTION

Current treatments for cancer rely on systemic administration of chemotherapeutic drugs with the goal of maximizing damage to tumor cells despite exposure and toxicity to healthy tissues. This approach is beneficial for damaging tumor tissue but due to the many side effects of these cytotoxic drugs, healthy tissues can be damaged and organ function can be compromised. Targeted delivery of drugs to tumors attempts to improve the bioavailability of drugs at the tumor site while reducing systemic toxicity to healthy organs and tissues. The efficacy of traditional cytotoxic cancer therapies comes with the price of significant toxicity to normal cells, which can limit the success of therapy. Greater understanding of the molecular differences between cancer cells and normal cells has led to the development of therapies that target cancer cells, including antibodies targeted at tumor associated antigens. The targeted nature of such therapies offers the promise of greater efficacy and less toxicity, and potentially greater treatment success.

## Vascular Targeting

Tumor angiogenesis is recognized as essential for the growth and progression of all tumor types, therefore, targeting the delivery of cytotoxic and radiosensitizing drugs to tumor blood vessels is an important approach in the treatment of cancer. The lumen of tumor microvasculature is composed of a monolayer of endothelial cells that controls vascular tone, blood flow and extravasation of components from the bloodstream [1]. This microvascular tissue plays an essential role in the process of inflammation and is affected by radiation therapy used in many cancer treatments. Radiation therapy is typically used to treat tumors locally, but it can also be used to "guide" drugs to specific sites by creating localized areas of inflammation and inducing the expression of radiation-specific receptors in tumors, including P-selectin [2,3]. Studies have shown that ionizing radiation causes oxidative injury in endothelial cells, which in turn respond by activating the process of inflammation and platelet aggregation through cell adhesion molecules (CAMs) [4,5,6]. These molecules include ICAM-1, VCAM, integrins, and selectins among others. Once vascular endothelium is exposed to ionizing radiation, proteins contained within storage reservoirs in endothelial cells are transported to the cell membrane, where they can serve as receptors for radiation-targeted drug delivery [2,3].

Tumor microvascular endothelium that has been exposed to radiation expresses many receptors that can be identified and targeted, including molecules in the selectin family [7]. These molecules are expressed on leukocytes (L-selectin), endothelial cells (E-selectin, P-selectin) and platelets (P-selectin). These cell adhesion molecules are known for mediating leukocyte rolling on endothelial cells and platelet-leukocyte

aggregation [9,10,11]. Studies have shown that elevated levels of selectins are present in the serum of subjects experiencing an inflammatory state [13]. P-selectin, in particular, is an important disease marker as it plays an essential role in many inflammatory processes including cancer, coronary artery disease, stroke, and diabetes [10,13]. It is also a valuable target for drug delivery because it is radiation-inducible, and its cellular expression is rapid and reversible [7,14]. Due to its increased expression on endothelial cells, its potential as a vascular target for tumor imaging and therapy has been proposed in this study.

## Radiation Induced P-selectin

Radiation therapy is needed to treat approximately 60% of patients with cancer [7]. Ionizing radiation induces the expression of cell adhesion molecules and other proteins in tumor microvasculature [7]. Targeting radiation-induced neoantigens on tumor microvasculature is a valuable approach for site-specific delivery of cytotoxic drugs and therapeutic radionuclides. We hypothesized that radiation-induced neoantigens such as P-selectin can be targeted with antibodies for tumor imaging and targeted drug delivery to cancer.

P-selectin (also designated as CD62P) is a 140 kD integral glycoprotein originally found on the surface of activated platelets (giving rise to the designation *P*-selectin) and later on endothelial cells [11,12]. It is sequestered in storage vesicles in the form of α-granules in platelets and Weibel-Palade bodies in endothelial cells [7,9]. Upon exposure to ionizing radiation, P-selectin expression is stimulated and these secretory granules fuse with the cell membrane [7]. Typically, this expression can also be induced

by the presence of various cytokines including histamine, thrombin, tumor necrosis factor alpha (TNFα) and lipopolysaccharide [7]. Once P-selectin is expressed on the surface of endothelial cells, it is rapidly internalized by endocytosis. Its general structure consists of an amino-terminal lectin domain, EGF-like domain, a variable number of short consensus repeat units, followed by a carboxyl-terminus [11].

After radiation exposure, P-selectin is transiently expressed on the vascular endothelial cells in the lumen of the vasculature, and once inflammation has subsided it moves back to the cell interior [7]. This transient expression enables the identification of a particular window of time during which targeting the tumor microvasculature can be particularly effective. This approach can be used to target both therapeutic and imaging agents to the radiation-treated tumor.

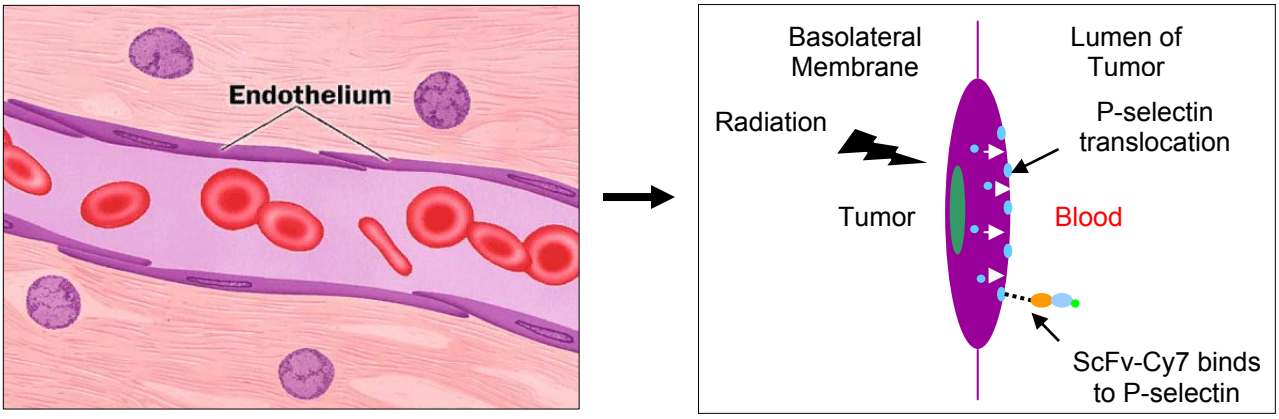


**Figure 1** Schematic of endothelial cell response to ionizing radiation.

In our study, we specifically examined the role of antibodies targeted to radiation-induced P-selectin in tumor microvasculature. This method of targeting tumors is significant

because antibodies can be produced to specifically bind P-selectin, which can then be conjugated to drugs and other therapeutics for radiation-guided drug delivery.

## Therapeutic Antibodies

The use of therapeutic antibodies as a treatment for cancer began with the discovery of the structure of antibodies and the development of hybridoma technology [15,16]. These advances provided the first reliable source of monoclonal antibodies (mAbs), and allowed for the specific targeting of many different types of tumors. Monoclonal antibodies have been used in oncologic applications since the late 1990s with the development of rituximab (Rituxan), trastuzumab (Herceptin) and gemtuzumab (Mylotarg) [16]. Since then, there has been an increase in the number of targeted antibody therapies available. Most of these therapies are based on whole, intact mAbs. While providing therapeutic value, these mAbs often exhibit slow clearance from the blood compartment to the tumor and are often too large to sufficiently penetrate the tumor tissue, thus limiting the efficacy of this type of therapy [17,18]. The Fc domain in these intact mAbs can also bind to cellular receptors and slow clearance times, creating systemic side effects [17].

One alternative to these problems has been the genetic engineering of antibody fragments such as single chain fragment variable (scFv) antibodies. These antibody fragments are comprised of immunoglobulin heavy chain and light chain variable regions that are connected by a short peptide linker. These antibody fragments retain the specific antigen-binding affinity of the parent mAb, while reducing some of the disadvantages associated with mAbs. Some of these advantages include their relatively

small size (~30 kD), which enables them to penetrate tumors more rapidly and increase renal clearance rates, and also their lack of an Fc domain which makes them less immunogenic [17-20]. These advantages make scFv antibodies potentially useful for both tumor imaging and therapy.

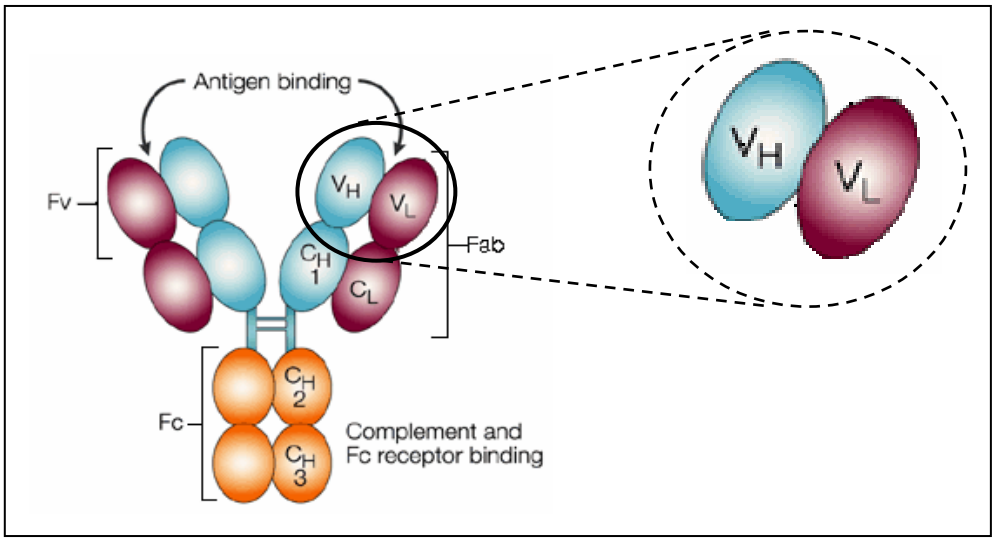


**Figure 2** Schematic of intact monoclonal antibody and single chain fragment variable region. Modified from Brekke et. al [16].

Radionuclides have also been used with therapeutic mAbs to either increase therapeutic activity or exploit the targeting properties of the mAbs for cancer imaging [21,22]. Radionuclide-bearing mAbs used in the clinic include Zevalin and Bexxar [21,22]. Although, such antibody therapies have shown significant success in cancer treatment, strategies to increase their efficacy are still needed. One approach has been to link antibodies against tumor associated antigens to highly toxic radionuclides to kill tumor cells [21,22]. Two examples of radiolabeled antibodies include Zevalin and Bexxar, both anti-CD20 mAbs radiolabelled with $^{90}Y$ and $^{131}I$, respectively [21,22].

The selection and characterization of anti-human P-selectin ScFvs is a first step toward the construction of cancer imaging or new anticancer antibodies designed for optimal blood clearance and tumor penetration. However, very few recombinant antibodies are available to study the clinical function of P-selectin except for therapeutic attempts in the form of monoclonal antibodies and chimeric antibodies [23-27]. Presently, there have not been any studies using P-selectin as an imaging target in cancer, partly due to the lack of specific desired antibodies to the protein. For these reasons, the aim of this study is to develop anti-human P-selectin scFvs that can be used for radiation-guided tumor imaging.

## Tumor Imaging

The ability to non-invasively visualize P-selectin targeting in vivo would allow us to understand the biodistribution and pharmacokinetics of antibodies conjugated drugs and radionuclides targeted to tumors. In this manner, tumor growth can be monitored and effectiveness of therapy can be evaluated. In this study, anti-P-selectin scFv antibodies have been labeled with fluorescent optical probes and radionuclides for near-infrared optical imaging and gamma camera imaging of P-selectin expression in radiation treated lung tumor xenografts. Tumor targeting efficacy and in vivo kinetics profiles were observed and evaluated using complementary optical and nuclear imaging modalities.

Nuclear imaging modalities such as PET, SPECT and gamma camera imaging typically exhibit high sensitivity in deep tissues but poor spatial and temporal resolution [35,36]. Optical imaging modalities have the advantage of higher resolution, safer

use since they do not use ionizing radiation or radioactive materials, but they provide lower sensitivity [28-32]. A major limitation of optical imaging is the high absorption and scattering that occurs in biological tissues and the consequently limited penetration of the light through the body. Near-infrared fluorescence (NIR) imaging is a particular kind of optical imaging that exploits the near-infrared range in the spectra to bypass the typical absorption and autofluorescence problems seen in optical imaging of biological tissues [28,29]. Typically, tissues exhibit a high photon absorbance in both the visible wavelength range (350-650 nm) and the infrared range (above 900 nm) [28]. However, in the NIR range of 650-900 nm the absorbance of water and tissues in the body is at a minimum and thus allows photons to penetrate tissue more efficiently and minimizes scattering [28-32]. Functional imaging of molecularly based events such as tumor-specific binding can be performed using both nuclear and optical imaging modalities in order to provide complementary information [33,34,37]. In this study, fluorescent probes in the NIR range were conjugated to anti-P-selectin scFvs for NIR optical imaging, and complementary data was gathered using $^{111}$In labeled anti-P-selectin scFvs with gamma camera imaging.

# CHAPTER II

# METHODS

Drug delivery methods generally rely on the use of targeting agents to deliver the conjugate to the appropriate site, and therapeutic agents to create the desired therapeutic effect at that site. In order to create optimal drug delivery vehicles, biodistribution and kinetics of the targeting agent and its receptor must first be studied and validated. Optical imaging and nuclear imaging are commonly used for these purposes and provide complementary information regarding targeting kinetics and biodistribution. This chapter focuses on the methods used for preliminary imaging studies in order to explore the potential of P-selectin targeting for radiation-guided drug delivery.

Experimental Setup

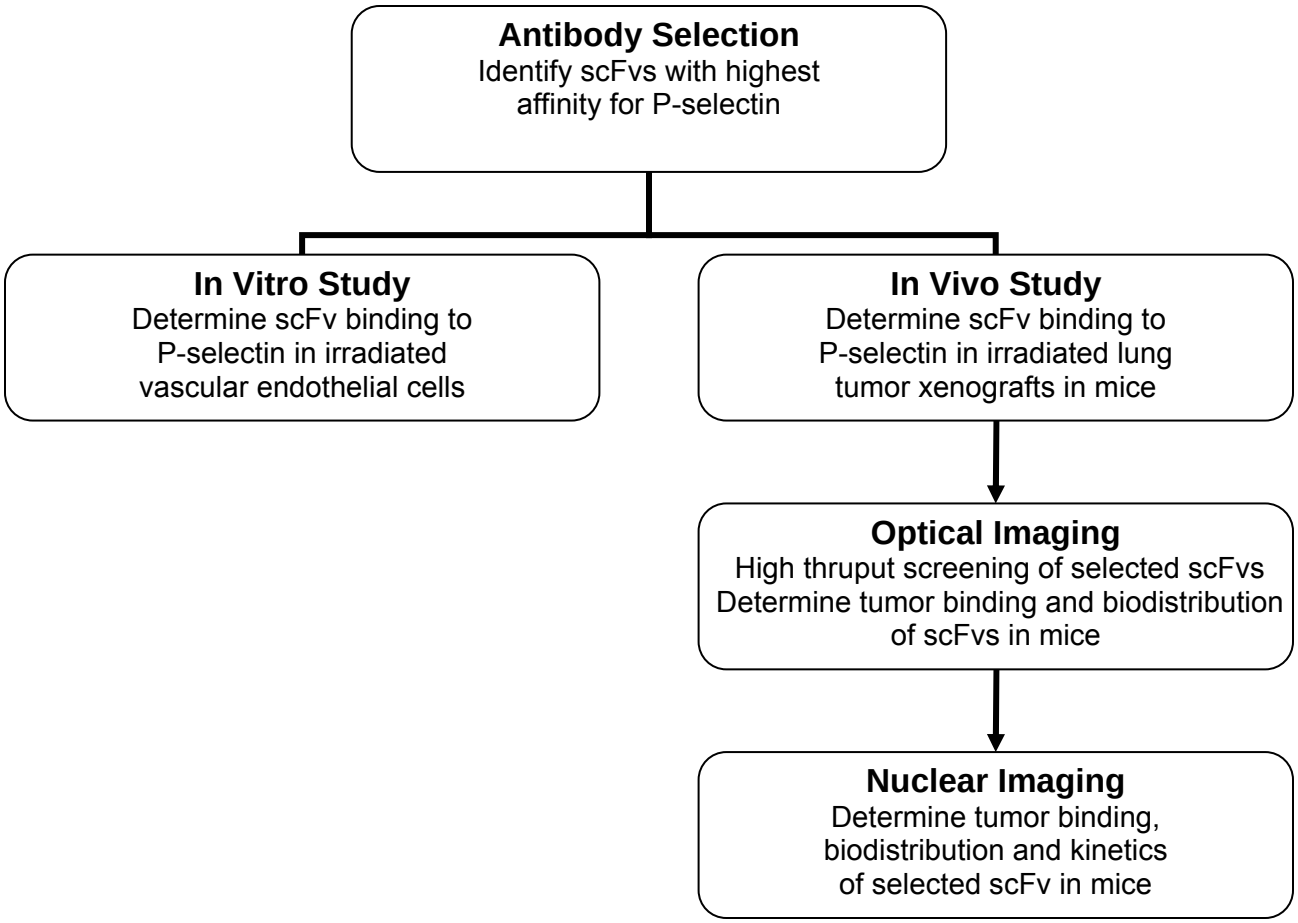

## Antibody Selection

All antibodies were screened from phage display libraries and developed in the Molecular Recognition Core Laboratory at Vanderbilt University. The antibodies with highest affinity for P-selectin were then selected for *in vitro* and *in vivo* imaging studies presented here. The modified antibody used in the nuclear imaging studies was developed in collaboration with Dr. Martin Brechbiel in the radiochemistry laboratory at the National Institutes of Health.

## In Vitro Model

### *Immunofluorescence Assay*

Primary culture human umbilical vein endothelial cells (HUVECs) were cultured till 80% confluency in Lab-Tek II chamber slide wells (Nunc International, Naperville, IL) in endothelial cell medium and incubated 37°C in a humidified 5% $CO_2$ atmosphere. Cells were then incubated with human TNFα (500 mM) for 30 minutes. After treatment, cells were fixed with 4% paraformaldehyde for 10 minutes at room temperature, and washed 3 times with antibody buffer (4 g bovine serum albumin, 0.1 g sodium azide, 0.75 g glycine, and 100 µl PBS at a pH of 7). All wells were blocked with 200 µl PBS containing 3% bovine serum albumin for 2 hs at room temperature. Anti-P-selectin scFv (100 µl) was added to selected wells and incubated at room

temperature for 1 hour in a humid chamber and then washed. The cells were incubated with 1 µg of biotinylated anti-E-Tag monoclonal antibody for 1 hour, washed 5 times with PBS-Tween solution and incubated with10 µl of a 1:200 dilution of Alexa Fluor 488 conjugated streptavidin for 1 hour. The cells were washed, counterstained with DAPI, and mounted with a solution of 90% glycerol and 10% PBS-Tween. Cells were visualized with an Olympus BX60 system for fluorescence microscopy. All images were obtained at an original magnification of 40x and imported and analyzed using Adobe Photoshop 7.0.

## In Vivo Model

### *Synthesis of ScFv-Cy7 Conjugates*

The synthesis of Cy7-scFv conjugates was achieved through conjugation of monofunctional Cy7-NHS ester with the ε-amino group of the lysine residue of the scFv antibody (Fig. 3). The reaction was performed in a sodium bicarbonate buffer at a pH of 8. The dye to scFv ratio was calculated to be 4:1. All scFv were labeled according to Amersham Biosciences protocol for labeling with Cy dye NHS esters. The resulting conjugates were purified using a gel desalting column (G-25, Pierce). The yields of Cy7-scFv conjugates were typically over 80%.

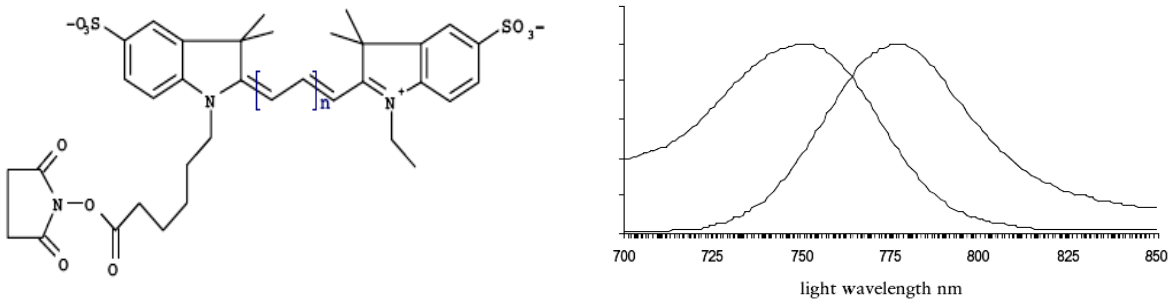


**Figure 3** Chemical structure and spectra of Cy7 fluorescent dye (Amersham) www.molecularprobes.com.

*Synthesis of $^{111}$In-DTPA-scFv10Acys Conjugates*

In order to radiolabel scFv 10A with $^{111}$In, a chelator (DTPA) was used for enhanced in vivo stability of the radionuclide (Fig. 4). To enable conjugation of scFv 10A to DTPA, a cysteine residue was engineered into the amino acid sequence of the scFv. The synthesis of $^{111}$In-DTPA-scFv10Acys conjugate was achieved through conjugation of scFv 10Acys-DTPA with $^{111}$In using thiol chemistry of the cysteine residue. The reaction was performed by adding 5 ul of $^{111}InCl_3$ (3 mCi) to the scFv 10Acys-DTPA conjugate in 120 ul of sodium citrate (1M) buffer (pH 5) and incubating at room temperature for 1 hr. The resulting conjugate was purified using a gel desalting column (G-25, Pierce). The yields of $^{111}$In-DTPA-scFv10Acys conjugate were typically over 70% as measured by thin layer chromatography.

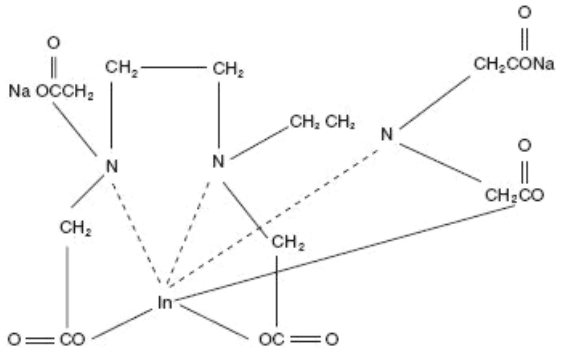


**Figure 4** Chemical structure of DTPA chelated $^{111}$In radionuclide (Amersham Health). www.amersham.com

*Cell Culture*

Lewis lung carcinoma (LLC) cells were obtained from American Type Culture Collection (Mannassas VA, USA) and were cultured at 37˚C in a humidified atmosphere containing 5% $CO_2$ in Dulbecco's modified eagle medium supplemented with 10% fetal bovine serum and 1% penicillin streptomycin solution.

*Animal Models*

Animal studies were performed according to a protocol approved by Vanderbilt's IACUC. Male athymic nude mice (nu/nu) between four to six weeks old (Harlan Inc., Indianapolis IN, USA) were anesthetized using a ketamine and xylazine solution before being injected subcutaneously in the right and left hind legs with 1 x $10^6$ LLC cells suspended in 100 µL sterile phosphate buffered saline. Ten days after inoculation, the tumors reached an approximate size of 0.5-0.6 cm in diameter, and the mice were used for *in vivo* imaging studies.

*Statistical Analysis*

One-way analysis of variance (ANOVA) was used for statistical evaluation. Means were compared by using Student's t-test. A p-value of $<0.05$ was considered significant.

*Radiation Treatment*

Mice were irradiated with 300kV X-rays using a Pantak Therapax 3 linear accelerator system (Pentak, East Haven, CT) using an adjustable collimator set to limit dosage to the tumor region only (Fig. 5). The animals were anesthetized using ketamine and xylazine solution prior to irradiation to inhibit mobility during treatment. The left hind limb was irradiated at a dose of 6 Gy and the right hind limb was treated with sham radiation at a dose of 0 Gy. During irradiation procedures, 1 cm thick lead blocks were arranged above the rest of the body, leaving only the desired area on the hind limb exposed for treatment.


**Figure 5** Linear accelerator used for radiation treatments.

## Optical Imaging

### *In vivo NIR Fluorescence Imaging*

In vivo NIR fluorescence imaging was performed with a Xenogen IVIS 200 small animal imaging system (Xenogen Inc., Alameda CA, USA) with a Cy7 filter set (excitation at 680 nm and emission at 775 nm). Nude mice bearing Lewis lung carcinoma tumors implanted in both hind limbs were treated with radiation. The tumor on the left side of each moused received a radiation dose of 6 Gy and the tumor on the right side received no radiation (sham radiation dose of 0 Gy) and served as an internal negative control. Three hours following radiation, mice were anesthetized using an intraperitoneal injection of ketamine and xylazine and prepared for tail vein injections of the scFv-Cy7 conjugates. The experimental group consisted of 3 mice receiving 50 µg of scFv 10A-Cy7, and the control group of consisted of 3 mice receiving 50 µg of scFv 4A-Cy7.

At 1, 4 and 8 hrs post-injection, all mice were anesthetized with isoflurane and imaged with the Xenogen IVIS. The surface fluorescence intensity of each animal was measured and normalized. All fluorescence images were acquired with one second exposure time using an f/stop of. Following imaging at the final time point, mice were immediately euthanized by inhalation of carbon dioxide, and their tumors and major organs were dissected and prepared for ex vivo imaging. The total fluorescence flux ($p/s/cm^2/sr$) for each organ was measured. For quantitative comparison,

regions of interest (ROIs) were drawn over tumors and normal tissues and the results were presented as mean ± standard deviation (SD) for a group of three animals.

## Nuclear Imaging

*In vivo Gamma Camera Imaging*

In vivo gamma camera imaging was performed with a large-field-of-view Starcam General Electric gamma camera (Fig. 6). Mice (n=3 for each $^{111}$In-DTPA-scFv conjugate) were anesthetized with ketamine/xylazine solution and injected via tail vein with 500 μCi of $^{111}$In-DTPA-scFv conjugate containing 50 μg scFv each. Planar images were taken every 24 hours after injection of the $^{111}$In-DTPA conjugated scFv antibody for 10 days. Static digital images were collected for 10 minutes each in a 512 x 512 matrix, with typical counts around 500,000 at the 24-hour imaging time and fewer counts with each subsequent imaging session. All images were processed using ImageJ software provided by the NIH. Following imaging of the final time point, mice were immediately euthanized by inhalation of carbon dioxide, and their tumors and major organs were dissected and individually labeled for well counts. The total counts for each organ were measured. For quantitative comparison, regions of interest (ROIs) were drawn over tumors and normal tissues in the planar images, and the results were presented as mean ± standard deviation (SD) for a group of three animals.

**Figure 6** General Electric gamma camera used.

# CHAPTER III

# RESULTS & DISCUSSION

## In Vitro Results

To determine whether scFv 10A bound to P-selectin *in vitro*, HUVECs were treated with TNF$\alpha$ to stimulate P-selectin expression on the cell membrane before being incubated with antibody. During immunofluorescent microscopy of the treated cells, it was observed that scFv 10A antibody bound to P-selectin protein on the cell membrane of cells treated with TNF$\alpha$ 30 minutes after treatment (Fig. 7). Control scFv antibody did not show significant antibody binding to P-selectin on the cell membrane (Fig. 7).

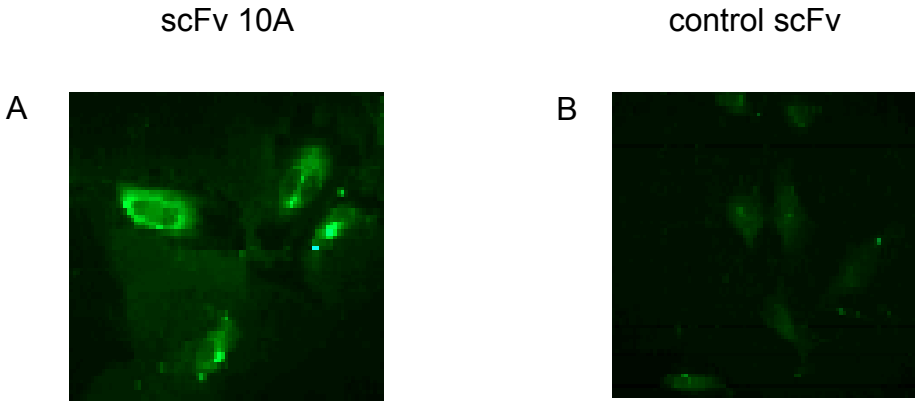


**Figure 7** Immunofluorescent microscopy of antibody binding to P-selectin in HUVECs treated with TNF$\alpha$.

To confirm whether scFv 10A bound to P-selectin *in vitro*, HUVECs were treated with ionizing radiation to stimulate P-selectin expression on the cell membrane before being incubated with antibody. Cells were stained with DAPI nuclear stain (blue) and scFv 10A was conjugated with Cy3 dye (red). During immunofluorescent microscopy of the treated cells, it was observed that scFv 10A antibody bound to P-selectin protein on the cell membrane of cells treated with a radiation dose of 3 Gy 30 minutes after treatment (Fig. 8 ). ScFv10A antibody did not show significant binding to cells treated with sham radiation of 0 Gy (Fig. 8 ).

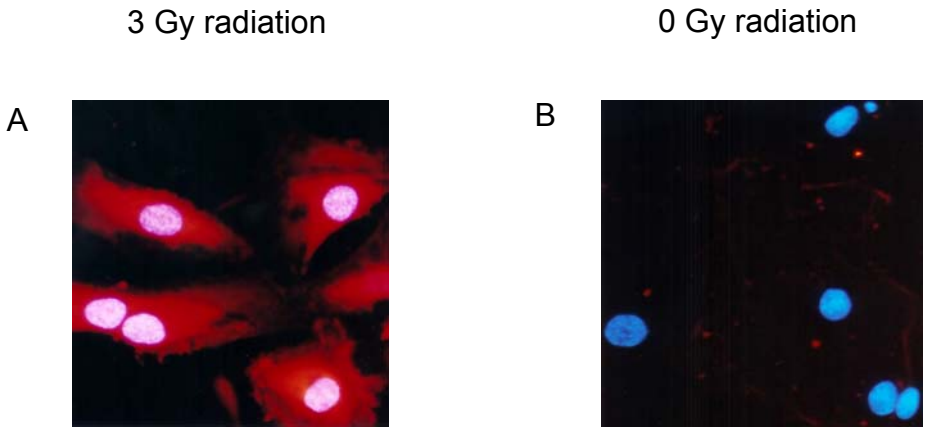


**Figure 8** Immunofluorescent microscopy of antibody binding to P-selectin in HUVECs treated with radiation.

In Vivo Model Results

*Optical Imaging*

To determine whether scFv 10A bound to P-selectin *in vivo*, nude mice with Lewis lung carcinoma xenografts were treated with radiation before receiving antibody. Near-infrared (NIR) fluorescence imaging studies were performed in order to evaluate the tumor targeting ability of scFv 10A as compared to control antibody scFv 4A (Fig. 9). Specific targeting was seen with scFv 10A to the tumor treated with 6 Gy (left leg) as compared to untreated tumor (right leg) and the rest of the body as early as 4 hours post-injection (Fig.9). Mice treated with scFv 4A did not show tumor-specific binding, with considerable antibody still circulating in the kidneys at 4 hrs post-injection.

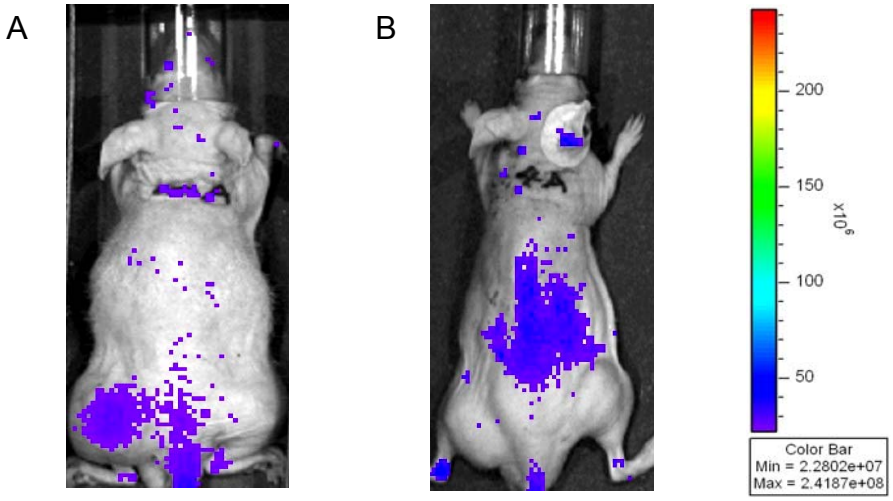


**Figure 9** NIR imaging of *in vivo* scFv biodistribution at 4 hrs post-injection.

The antibody biodistribution in the animal was tracked using near-infrared imaging at 4 hours after injection. Fluorescence intensity of different regions of interest (ROI) was created by quantifying photons emitted per second for each desired area. The ratios of irradiated tumor, control tumor and the rest of the body per kilogram of body weight are shown (Fig. 10). The ratio of fluorescence intensity of the irradiated tumor to the control tumor is approximately 25:1, and the ratio to the rest of the body is over 100:1.

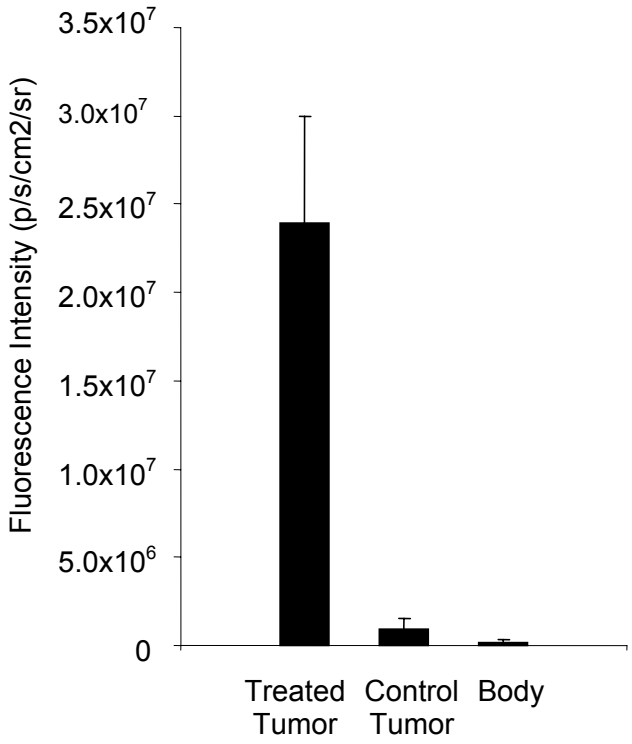


**Figure 10** Graph of tumor to body ratios from NIR imaging

In order to confirm tumor binding of scFv 10A, tumors were excised and imaged ex vivo (Fig. 11). The irradiated tumor shows significantly more fluorescence intensity as compared to the unirradiated control ScFv 4A exhibits no tumor binding.

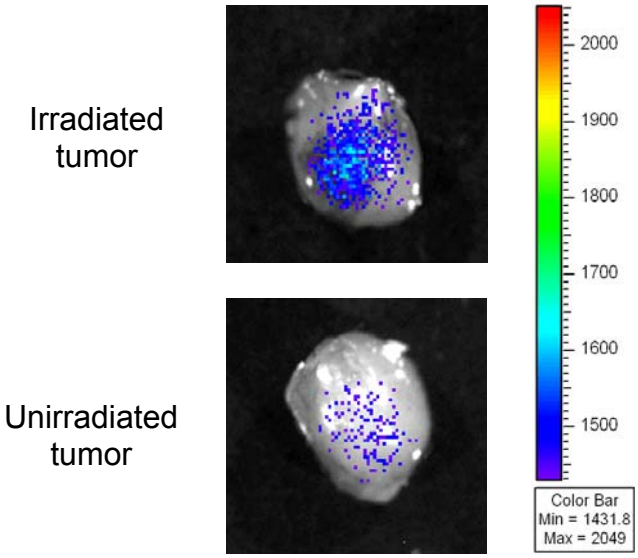


**Figure 11** NIR imaging of ex vivo scFv 10A in tumors treated with and without radiation at 4 hours post-injection.

*Nuclear Imaging*

To evaluate the P-selectin targeting ability of scFv 10A in vivo, and validate the results observed in the near-infrared fluorescence imaging studies, gamma camera imaging studies were performed using the γ ray emitting radionuclide $^{111}$In. In order to do this, a chelator (DTPA) was used to sequester the $^{111}$In and enhance stability in vivo. The scFv 10A antibody was also modified to contain a cysteine residue (scFv 10Acys) in order to allow conjugation of the DTPA chelated $^{111}$In.

To determine whether scFv 10Acys bound to P-selectin *in vivo*, nude mice bearing Lewis lung carcinoma tumors were treated with the tumor on the left side of each animal receiving a radiation dose of 6 Gy and the tumor on the right side receiving an intratumoral injection of TNFα as an internal positive control. Negative controls consisted of mice with tumors that were treated with no radiation (sham radiation dose of 0 Gy). Three hours following radiation, $^{111}$In-DTPA conjugated scFv 10Acys was injected into both groups of mice.

Beginning 24 hours after injection all mice were imaged on a gamma camera imaging system at 24 hours post-injection and every 24 hours after for up to 10 days (or approximately 3 half-lives for the $^{111}$In). Specific targeting was seen with scFv 10Acys to the tumor treated with 6 Gy (left leg) and the tumor treated with TNF$\alpha$ as compared to untreated control tumors. Binding was observed at 24 hours and continued for up to 10 days post-injection. Figure 12 shows a representative image of $^{111}$In-DTPA conjugated scFv

10Acys targeting a Lewis lung carcinoma tumor treated with 6 Gy showing tumor targeting for up to 10 days after injection.

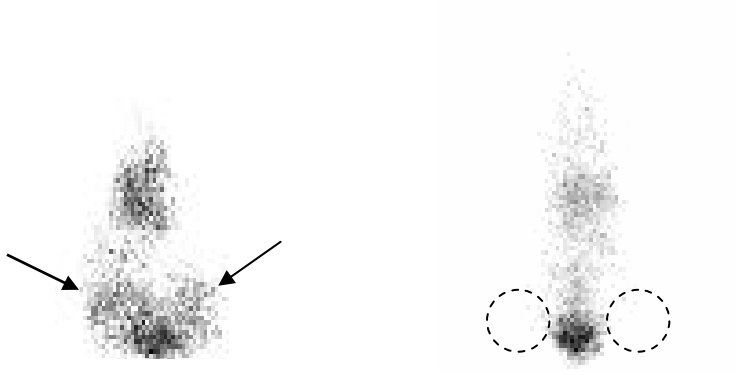

**Figure 12** Gamma camera imaging of *in vivo* scFv biodistribution at 10 days post-injection.

Figure 13 below shows a higher percentage (>10%) of binding activity in tumors treated with 6 Gy radiation than tumors treated with TNFα. Binding activity dropped approximately 30% in radiation-treated tumors over a period of ten days. Binding activity in TNFα treated tumors decreased approximately 45% over ten days. Both radiation-treated and TNFα treated tumors showed increased tumor binding activity over tumors treated with sham radiation of 0 Gy.

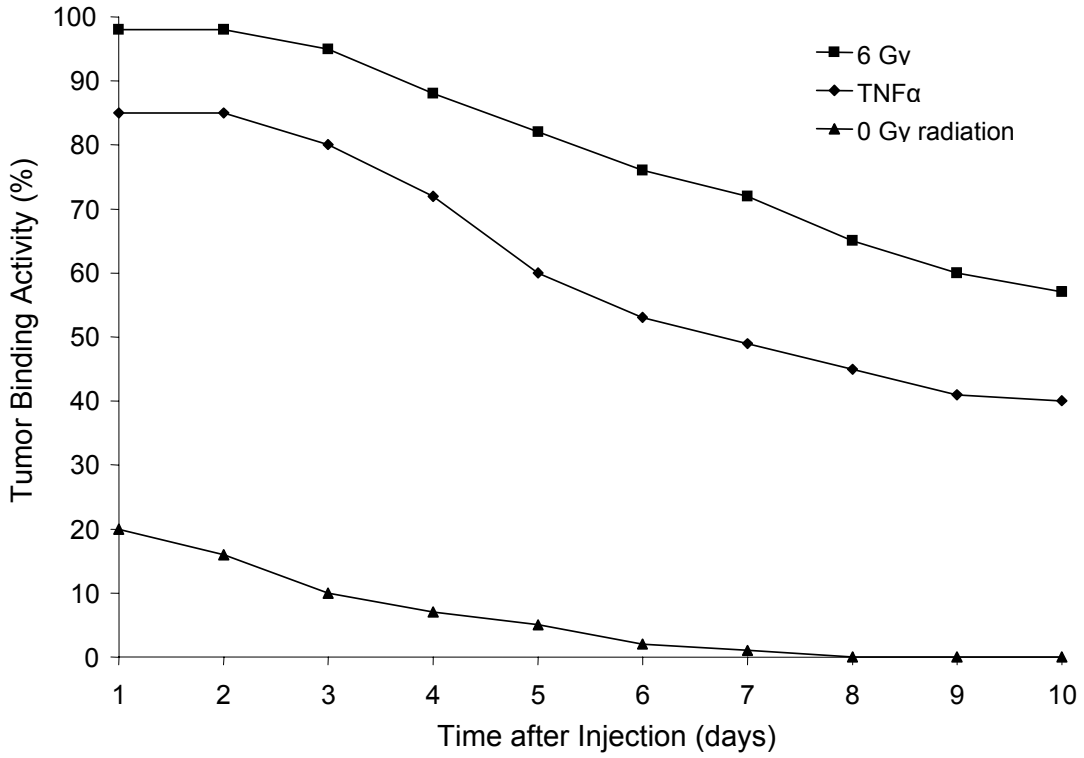


**Figure 13** Tumor binding activity of three different treatments with a gamma camera.

ScFv 10Acys binds tumors in vivo treated with both radiation and TNFα treatment for up to 10 days post-injection (Fig. 14). However, radiation produced greater P-selectin binding than TNFα. Tumor binding was nearly five times higher in radiation treated tumors as compared to untreated tumors. Tumor binding remained constant for up to two days before steadily decreasing up to ten days. As expected, percent uptake was highest in the liver, followed by radiation treated tumor, kidneys, bladder, TNFα treated tumor, and untreated tumor. Liver, kidney and bladder uptake decreased by approximately half over a time period of ten days.

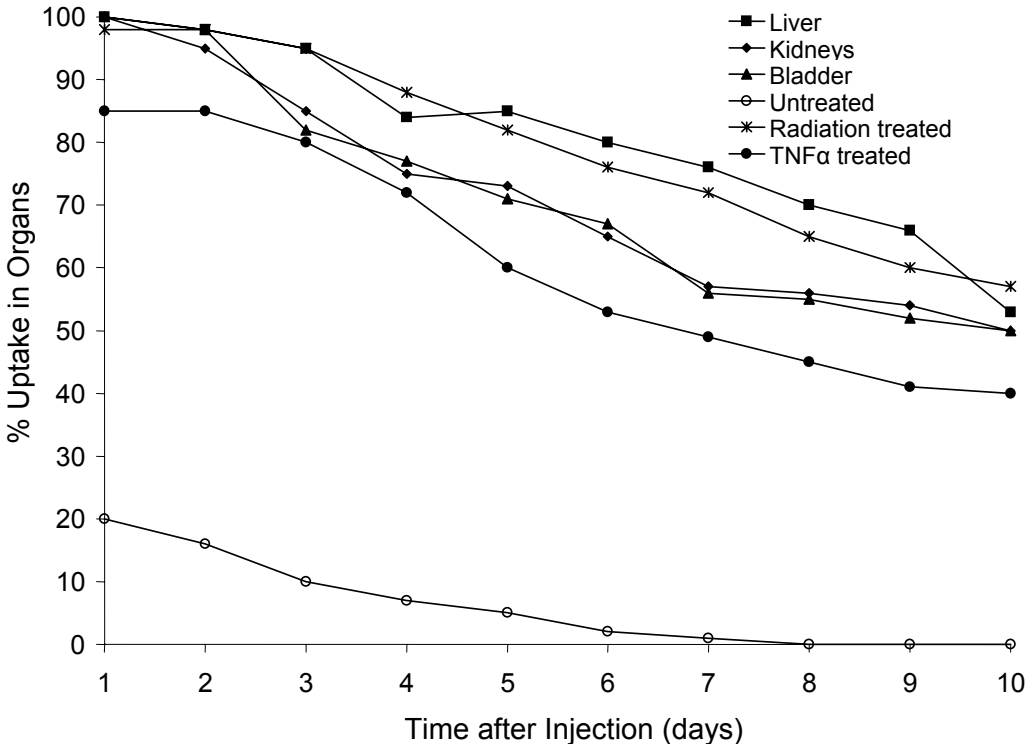


**Figure 14** Percent uptake of $^{111}$In-DTPA-scFv 10Acys in various organs over 10 days after injection as measured with a gamma camera.

## Discussion

Expression of P-selectin in tumor vascular endothelium after exposure to ionizing radiation enables the preferential delivery of labeled anti-P-selectin scFv antibodies to irradiated tumors. Previous studies with radiolabeled scFv demonstrated the site-specific localization of the antibodies in the targeted tumor vascular cells. In our study, we described the selective targeting of scFv antibodies to tumors in vivo using two methods: NIR fluorescence imaging and gamma camera imaging. Near-infrared (NIR) imaging is a useful non-invasive tool for visualizing tumor targeting in vivo, and a powerful complement to nuclear imaging techniques. NIR imaging has the advantages of using neither ionizing radiation nor radioactive materials, and is becoming a more important tool for imaging of animals in preclinical models. Fluorescent probes, such as Cy7, allow the visualization of anatomical, functional and molecular events in small animals. These attributes make it ideal for studying the molecular target P-selectin and its role in tumor vasculature. With better understanding of tumor angiogenesis, it is possible to develop P-selectin targeted therapies. To achieve this, imaging studies with both NIR and nuclear techniques were performed and tumor targeting to P-selectin was studied. NIR fluorescence imaging was performed using a Cy7-conjugated scFv antibody, and gamma camera imaging was performed using an $^{111}$In-DTPA-conjugated scFv antibody modified to include a cysteine residue for conjugation purposes. Combining both optical imaging and nuclear imaging

techniques enabled the confirmation of results using complementary imaging modalities.

Optical imaging techniques such as NIR fluorescence imaging take advantage of recent developments in fluorescent probes in the near-infrared region of the spectrum. Conjugation of Cy7, a fluorescent probe with excitation at 680 nm and emission at 775 nm, did not have significant effect on the optical properties of Cy7 dye and did not affect the receptor binding affinity or specificity of the scFv antibodies to P-selectin. Since NIR fluorescence intensity is a function of optical path length between excitation light and the subject, subcutaneous tumor models were chosen for this study. Imaging was done both in vivo and ex vivo with excised tumors in order to validate signal detected in *in vivo* images. As expected, fluorescence intensity was lesser *in vivo* as compared to direct imaging of dissected tissues. Other researchers have noted similar observations when imaging with and without skin and detected an attenuation of fluorescence intensity by approximately 44% [32]. This is most likely caused by the loss of excitation and emission light by penetration of the skin, in addition to scattering caused by the skin. Because of these issues, gamma camera imaging was used to minimize the effects of skin scattering on imaging of tumor binding.

The binding of labeled scFv antibody to P-selectin was tested using in vitro and in vivo techniques. Human umbilical vein endothelial cells (HUVECs) treated with TNFα, a potent stimulator of P-selectin, were incubated in the presence of scFv antibody and immunostained showing binding to P-selectin

present on cells. Cell staining was observed all over the cell membrane, consistent with the observed location of P-selectin after TNF$\alpha$ and radiation treatment [7]. Staining of cell membranes was not present when scFv not specific to P-selectin (control scFv) was used. Immunofluorescence confirms that scFv 10A antibody selectively binds to HUVEC cells expressing P-selectin and does not bind to other cells. Therefore, we have successfully demonstrated that scFv 10A antibody is specific to human P-selectin expressed on the surface of vascular endothelium.

In vivo NIR fluorescence imaging of mice with irradiated and unirradiated tumors given Cy7-labeled scFv 10A and 4A showed significant targeting of irradiated tumors using scFv 10A as early as 4 hours post treatment. Binding in tumors was measured to be over 25 times higher than in unirradiated tumors and over 100 times higher than the rest of the body. Direct imaging of excised tumors confirmed these results with significant binding in irradiated tumors as compared to unirradiated tumors. Tumor binding was not observed in animals treated with scFv 4A.

In order to further study the kinetics of this scFv antibody, the antibody was modified to include a cysteine residue for conjugation to DTPA and was then radiolabeled with $^{111}$In, a gamma emitter. This modified antibody construct was used to image mice with irradiated tumors, TNF$\alpha$ treated tumors and unirradiated tumors. The ionizing gamma rays emitted from the $^{111}$In penetrated through the tumor and surrounding layers of skin, providing greater sensitivity with gamma camera imaging as compared to NIR

fluorescence imaging. In vivo imaging showed significant accumulation of radiolabelled scFv 10Acys in irradiated tumor tissue as compared to TNFα treated tumors, unirradiated tumors and the rest of the body for up to 10 days post-injection. Our data show that scFv 10Acys selectively targets P-selectin in vivo as induced with both radiation and TNFα treatment at 10 days post-injection. However, radiation produced greater P-selectin binding than TNFα. Tumor binding was nearly five times higher in radiation treated tumors as compared to untreated tumors, again suggesting antibody binding to be higher in P-selectin expressing tumors. Biodistribution of the scFv 10Acys antibody showed higher uptake in the liver, kidneys and bladder as compared to tumors treated with radiation, TNFα, and no treatment. Percent uptake was highest in the liver due to processing by macrophages, followed by radiation treated tumor, kidneys, bladder, TNFα treated tumor, and untreated tumor.

## Future Work

Imaging P-selectin targeting in vivo provides a stepping stone to achieving radiation-guided drug delivery to P-selectin expressing tumors in vivo. Follow up work in this area would include the investigation of therapeutic radionuclides and compatible chelators that could be linked to the identified antibody scFv 10A. Effects on tumor growth must be studied over time to determine if this approach produces therapeutic effects. In addition, safety and toxicity studies must be done to determine the effects of these radionuclides on vital organs over time. Targeted drug delivery to P-selectin in irradiated tumors should be studied using chemotherapeutic and radiosensitizing drugs commonly used in radiation therapy. Combining tumor imaging with targeted drug delivery would enable important parameters such as biodistribution, pharmacokinetics and bioavailability to be studied in more detail. By using the targeting capability of antibodies, and exploiting the side-effects of radiation therapy, it is possible to target and treat tumors locally with both radiation and chemotherapeutic drugs much more effectively.

# CHAPTER IV

## CONCLUSIONS

In this study we have demonstrated the successful non-invasive *in vivo* targeting of an antibody to radiation-inducible neoantigen P-selectin, in a heterotopic Lewis lung carcinoma model by using near-infrared fluorescence imaging and gamma camera imaging. In our preliminary optical imaging study, it was observed that tumor-specific binding was seen as early as 4 hours post-injection. Binding in irradiated tumors was over 25 times higher than in unirradiated tumors and over 100 times higher than the rest of the body. It was also shown that scFv 10A binds P-selectin in TNF$\alpha$ and radiation treated HUVECs in vitro. Gamma camera imaging showed that the modified scFv 10A also showed successful targeting to P-selectin with tumor binding lasting for up to 10 days post-injection. Therefore, radiation-guided targeting of P-selectin for the tumor-specific delivery of therapeutic drugs and radionuclides in vivo is a feasible approach.

# REFERENCES


1. Lin P.C. Optical imaging and tumor angiogenesis. Journal of Cellular Biochemistry 2003;90:484-491.

2. Hallahan D.E., Qu S., Geng L., Cmelak A., Chakravarthy A., Martin W., Scarfone C., and Giorgio T. Radiation-mediated control of drug delivery. American Journal of Clinical Oncology 2001;24(5):473-480.

3. Hallahan D.E., Geng L., Cmelak A.J., Chakravarthy A.B., Martin W., Scarfone C., Gonzalez A. Targeting drug delivery to radiation-induced neoantigens in tumor microvasculature. Journal of Controlled Release 2001;74:183-191.

4. Hallahan D., Geng L., Qu S., Scarfone C., Giorgio T., Donnelly E., Gao X., and Clanton J. Integrin-mediated targeting of drug delivery to irradiated tumor blood vessels. Cancer Cell 2003;3:63-74.

5. Geng L., Osusky K., Konjeti S., Fu A., and Hallahan D. Radiation-guided drug delivery to tumor blood vessels results in improved tumor growth delay. Journal of Controlled Release 2004;1-13.

6. Barcellos-Hoff M.H., Park C., and Wright E.G. Radiation and the microenvironment – tumorigenesis and therapy. Nature Reviews Cancer 2005;5:867-875.

7. Hallahan D.E., and Virudachalam S. Accumulation of P-selectin in the lumen of irradiated blood vessels. Radiation Research 1999;152:6-13.

8. Wachsberger P., Burd R., and Dicker A.P. Tumor response to ionizing radiation combined with antiangiogenesis or vascular targeting agents: exploring mechanisms of interaction. Clinical Cancer Research 2003;9:1957-1971.

9. Dole V.S., Bergmeier W., Mitchell H.A., Eichenberger S.C., Wagner D.D. Activated platelets induce Weibel-Palade-body secretion and leukocyte rolling in vivo: role of P-selectin. Blood 2005;106(7):2334-2339.

10. Lorant D.E., Topham M.K., Whatley R.E., McEver R.P., McIntyre T.M., Prescott S.M., Zimmerman G.A. Inflammatory roles of P-selectin. Journal of Clinical Investigation 1993;92(2):559-570.

11. McEver R.P. Selectins. Current Opinions in Immunology 1994;6(1):75-84.

12. McEver R.P. Regulation of function and expression of P-selectin. Agents Actions Supplement 1995;47:117-119.

13. Molenaar T.J.M., Twisk J., de Haas S.A.M., Peterse N., Vogelaar B.J.C.P, van Leeuwen S.H., Michon I.N., van Berkel T.J.C., Kuiper J., and Biessen E.A.L. P-selectin as a candidate target in atherosclerosis. Biochemical Pharmacology 2003;66:859-866.

14. Kneuer C., Ehrhardt C., Radomski M.W. and Bakowsky U. Selectins – potential pharmacological targets? Drug Discovery Today 2006;11:1034-1040.

15. McCarron P.A., Olwill S.A., Marouf W.M.Y., Buick R.J., Walker B., and Scott C.J. Antibody conjugates and therapeutic strategies. Molecular Interventions 2006;6(2):368-380.

16. Brekke O.H. and Sandlie I. Therapeutic antibodies for human diseases at the dawn of the twenty-first century. Nature Reviews Drug Discovery 2003;2:52-62.

17. Wu A.M., and Senter P.D. Arming antibodies: prospects and challenges for immunoconjugates. Nature Biotechnology 2005;23(9):1137-1146.

18. Lin M.Z., Teitell M.A., and Schiller G.J. The evolution of antibodies into versatile tumor-targeting agents. Clinical Cancer Research 2005;11:129-138.

19. Carter P. Improving the efficacy of antibody-based cancer therapies. Nature Reviews Cancer 2001;1:118-129.

20. Fang J., Jin H., and Song J. Construction, expression and tumor targeting of a single-chain Fv against human colorectal carcinoma. World Journal of Gastroenterology 2003;9(4):726-730.

21. Milenic D.E., Brady E.D., and Brechbiel M.W. Antibody-targeted radiation cancer therapy. Nature Reviews Drug Discovery 2004;3:488-498.

22. Milenic D.E. and Brechbiel M.W. Targeting of radio-isotopes for cancer therapy. Cancer Biology and Therapy 2004;3(4):361-370.

23. Tsurushita N, Fu H, Melrose J, Berg EL. Epitope mapping of mouse monoclonal antibody EP-5C7 which neutralizes both human E- and P-selectin. Biochem Biophys Res Commun. 1998 6;242(1):197-201.

24. Walter UM, Ayer LM, Wolitzky BA, Wagner DD, Hynes RO, Manning AM, Issekutz AC. Characterization of a novel adhesion function blocking monoclonal antibody to rat/mouse P-selectin generated in the P-selectin-deficient mouse. Hybridoma. 1997 ;16(3):249-57.

25. He XY, Xu Z, Melrose J, Mullowney A, Vasquez M, Queen C, Vexler V, Klingbeil C, Co MS, Berg EL. Humanization and pharmacokinetics of a monoclonal antibody with specificity for both E- and P-selectin. J Immunol. 1998 15;160(2):1029-35.

26. Kurome T, Katayama M, Murakami K, Hashino K, Kamihagi K, Yasumoto M, Kato I. Expression of recombinant mouse/human chimeric antibody specific to human GMP-140/P-selectin. J Biochem (Tokyo).1994 ;115(3):608-14.

27. Gu J, Liu Y, Xia L, Wan H, Li P, Zhang X, Ruan C. Construction and expression of mouse-human chimeric antibody SZ-51 specific for activated platelet P-selectin. Thromb Haemost. 1997;77(4):755-9.

28. Chen X., Conti P.S., Moats R.A. In vivo near-infrared fluorescence imaging of integrin $\alpha_v\beta_3$ in brain tumor xenografts. Cancer Research 2004;64:8009-8014.

29. Wu Y., Cai W., Chen X. Near-infrared fluorescence imaging of tumor integrin $\alpha_v\beta_3$ expression with Cy7-labeled RGD multimers. Molecular Imaging and Biology 2006;8:226-236.

30. Hsu A.R., Hou L.C., Veeravagu A., Greve J.M., Vogel H., Tse V., and Chen X. In vivo near-infrared fluorescence imaging of integrin $\alpha_v\beta_3$ in an orthotopic glioblastoma model. Molecular Imaging and Biology 2006;8:315-323.

31. Cheng Z., Wu Y., Xiong Z., Gambhir S.S., and Chen X. Near-infrared fluorescent RGD peptides for optical imaging of integrin $\alpha_v\beta_3$ expression in living mice. Bioconjugate Chemistry 2005;16:1433-1441.

32. Zaheer A., Lenkinski R.E., Mahmood A., Jones A.G., Cantley L.C., and Frangioni J.V. In vivo near-infrared fluorescence imaging of osteoblastic activity. Nature Biotechnology 2001;19:1148-1154.

33. Lyons S. Advances in imaging mouse tumour models in vivo. Journal of Pathology 2005;205:194-205.

34. Dharmarajan S., and Schuster D.P. Molecular imaging of the lungs. Academic Radiology 2005;12:1394-1405.

35. Li C., Wang W., Wu Q., Ke S., Houston J., Sevick-Muraca E., Dong L., Chow D., Charnsangavej C. and Gelovani J.G. Dual optical and nuclear imaging in human melanoma xenografts using a single targeted imaging probe. Nuclear Medicine and Biology 2006;33:349-358.

36. Kundu B.K., Stolin A.V., Pole J., Baumgart L., Fontaine M., Wojcik R., Kross B., Zorn C., Majewski S., and Williams M.B. Tri-modality small animal imaging system. IEEE Transactions on Nuclear Science 2006;53(1):66-70.

37. Neves A.A., and Brindle K.M. Assessing responses to cancer therapy using molecular imaging. Biochimica et Biophysica Acta 2006;1766:242-261.